JACS
JOURNAL OF THE AMERICAN CHEMICAL SOCIETY
Article
pubs.acs.org/JACS

$Sc_2S@C_s(10528)$-C_{72}: A Dimetallic Sulfide Endohedral Fullerene with a Non Isolated Pentagon Rule Cage

Ning Chen,[†] Christine M. Beavers,[‡] Marc Mulet-Gas,[∥] Antonio Rodríguez-Fortea,[∥] Elias J. Munoz,[†] Yu-Yang Li,[†] Marilyn M. Olmstead,*[,§] Alan L. Balch,*[,§] Josep M. Poblet,*[,∥] and Luis Echegoyen*[,†]

[†]Department of Chemistry, University of Texas at El Paso, El Paso, Texas 79968, United States
[‡]Advanced Light Source, Lawrence Berkeley Laboratory, One Cyclotron Road, Berkeley, California 94720, United States
[§]Department of Chemistry, University of California, One Shields Avenue, Davis, California 95616, United States
[∥]Departament de Química Física i Inorgànica, Universitat Rovira i Virgili, c/Marcel·lí Domingo s/n, 43007 Tarragona, Spain

Supporting Information

ABSTRACT: A non isolated pentagon rule metallic sulfide clusterfullerene, $Sc_2S@C_s(10528)$-C_{72}, has been isolated from a raw mixture of $Sc_2S@C_{2n}$ (n = 35−50) obtained by arc-discharging graphite rods packed with Sc_2O_3 and graphite powder under an atmosphere of SO_2 and helium. Multistage HPLC methods were utilized to isolate and purify the $Sc_2S@C_{72}$. The purified $Sc_2S@C_s(10528)$-C_{72} was characterized by mass spectrometry, UV−vis−NIR absorption spectroscopy, cyclic voltammetry, and single-crystal X-ray diffraction. The crystallographic analysis unambiguously elucidated that the C_{72} fullerene cage violates the isolated pentagon rule, and the cage symmetry was assigned to $C_s(10528)$-C_{72}. The electrochemical behavior of $Sc_2S@C_s(10528)$-C_{72} shows a major difference from those of $Sc_2S@C_s(6)$-C_{82} and $Sc_2S@C_{3v}(8)$-C_{82} as well as the other metallic clusterfullerenes. Computational studies show that the Sc_2S cluster transfers four electrons to the C_{72} cage and $C_s(10528)$-C_{72} is the most stable cage isomer for both empty C_{72}^{4-} and $Sc_2S@C_{72}$, among the many possibilities. The structural differences between the reported fullerenes with C_{72} cages are discussed, and it is concluded that both the transfer of four electrons to the cage and the geometrical requirements of the encaged Sc_2S cluster play important roles in the stabilization of the $C_s(10528)$-C_{72} cage.

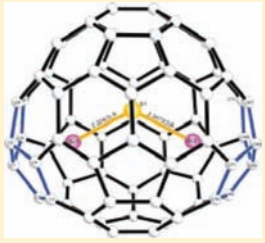

INTRODUCTION

Endohedral fullerenes have attracted much attention during the past few decades because of their unique host−guest structure.[1−7] The interior of the carbon cage provides a unique nanometer-scale space for the stabilization of some unstable clusters, while cages which do not obey the isolated pentagon rule (IPR) can also be stabilized by charge transfer from the encaged atom or clusters.[8−15] The structural variety of both the cages and the clusters gives rise to extreme versatility to alter their physical and chemical properties. Endohedral fullerenes are potentially useful as MRI contrast agents and in molecular electronic devices and solar cells.[4,5,7,16−28]

The encaged species can be metallic or nonmetallic atoms, small molecules, or metallic clusters.[1,6,17] In 1999, the first clusterfullerene, $Sc_3N@I_h$-C_{80}, was reported in exceptionally high yields, making it the third most abundant fullerene to date after C_{60} and C_{70}.[29] Since the discovery of $Sc_3N@I_h$-C_{80}, nitride clusterfullerenes (NCFs) have been successfully synthesized with scandium, yttrium, and most of the lanthanides, with cages ranging from C_{68} to C_{96}.[13,14,30−36] Different from NCFs, which only have trimetallic nitride template (TNT) clusters encaged in all of them, carbide clusterfullerenes (CCFs) show more structural versatility, including moieties such as Sc_xC_2 (x = 2−4), Sc_3CH, and Sc_3CN, with cages ranging from C_{68} to C_{92}.[11,37−40] The structural diversity gives rise to many unusual properties. For example, the CCF with the largest encapsulated cluster, $Sc_4C_2@C_{80}$, was found to have a Russian-doll-like structure, $C_2@Sc_4@C_{80}$.[38] Similar to CCFs, the oxide clusterfullerenes (OCFs) also demonstrate a variety of cluster structures, including Sc_2O, Sc_4O_2, and Sc_4O_3.[41−44] Among them, $Sc_4O_3@C_{80}$, with a seven-atom encaged cluster, is the largest cluster found in the clusterfullerene family to date.[41]

Very recently, a new family of clusterfullerenes, sulfide clusterfullerenes (SCFs), was discovered using different synthetic methods. Dunsch and co-workers reported the formation of one isomer of $M_2S@C_{82}$ (M = Sc, Lu, Dy) by introducing CH_5N_3·HSCN as a solid sulfur source.[45] We also demonstrated that an extensive family of novel SCFs with cages ranging from C_{80} to C_{100} can be obtained in macroscopic quantities by introducing SO_2 instead of a solid compound as the sulfur source.[46] Two isomers of $Sc_2S@C_{82}$ ($Sc_2S@C_s(6)$-C_{82} and $Sc_2S@C_{3v}(8)$-C_{82}) were identified as the most abundant products in this family and were recently characterized by single-crystal X-ray crystallography.[47]

Among the numerous endohedral fullerenes, the study of clusterfullerenes that do not obey the IPR is particularly interesting because of the match required between the cluster and the host cage.[8,48,49] The number of IPR cage isomers is always limited, but the number of possible non-IPR isomers can often be in the thousands as the cage sizes increase. Interestingly, with certain endohedral clusters and cage sizes,

Received: January 23, 2012
Published: April 21, 2012

   dx.doi.org/10.1021/ja300765z | J. Am. Chem. Soc. 2012, 134, 7851−7860

out of thousands of possibilities, there is frequently only one match between a particular cage isomer and the cluster.[48] Medium-size cages, such as $Gd_3N@C_s(39663)$-C_{82}[49] and $M_3N@C_s(51365)$-C_{84} (M = Gd, Tb, Tm),[15] were found to have a single pair of fused pentagons. Smaller cages, such as $Gd_3N@C_2(22010)$-C_{78},[12] $Sc_2@C_{2v}(4348)$-C_{66},[8] and $Sc_2C_2@C_{2v}(6073)$-C_{68},[50] possess two pairs of fused pentagons. Endohedral fullerenes that have three pairs of fused pentagons were also found for cages no larger than C_{70}, i.e., $Sc_3N@C_{2v}(7854)$-C_{70}[14] and $Sc_3N@D_3(6140)$-C_{68}.[13] These cages are not stable when empty and are stabilized by charge transfer from the encaged cluster. All these non-IPR endohedrals have the common feature that the internal metal ions are positioned in close proximity to the adjacent pentagon pairs.

Up to now, all empty fullerenes isolated obey the IPR. Non-IPR isomers have been identified for some endohedral systems and for some exohedrally derivatized cages. The only exception is C_{72}. Although it has an IPR isomer with D_{6d} symmetry, theoretical calculations suggest that this isomer is only the second most stable after the non-IPR isomer $C_{2v}(11188)$-C_{72}.[51,52] Hence, among cages ranging from C_{70} to C_{92}, C_{72} is the only empty fullerene which has never been isolated and characterized as an IPR isomer.[53,54] Up to date, three isomers of C_{72}, $La@C_2$-C_{72}[10] $La_2@D_2(10611)$-C_{72},[55] and $C_{2v}(11188)$-$C_{72}Cl_4$,[53,54] have been isolated and characterized. $C_{72}Cl_4$ utilizes the $C_{2v}(11188)$-C_{72} cage, which was predicted to be the most stable cage for pristine C_{72} fullerenes.[10,53,54,56,57] These observations suggest that the most energetically favorable C_{72} cage is not stable in its pristine form and needs to be buttressed by chlorination. The structure of $La@C_{72}$ and $La_2@C_{72}$ had to be determined after derivatization.[10,57] Thus, it is interesting to know if a C_{72} cage could be stabilized only by endohedral interactions and if so what kind of cage symmetry it would possess. Herein, we report the isolation of a metallic clusterfullerene in a C_{72} cage, $Sc_2S@C_{72}$. Crystallography clearly establishes that the C_{72} cage has an unusual $C_s(10528)$ symmetry which was proposed on the basis of theoretical calculations by Dunsch et al. for $Sc_3N@C_{72}$, but has never been detected experimentally previously.[58] Computational studies revealed that a formal charge transfer of four electrons of $Sc_2S@C_s(10528)$-C_{72} occurs between the cluster and the cage.

RESULTS

Preparation and Purification of $Sc_2S@C_{72}$. The SCFs were synthesized in a conventional Krätschmer–Huffman reactor using a mixture of helium and SO_2 atmosphere.[46,59] The as-produced soot was Soxhlet-extracted with CS_2, and a multistage high-performance-liquid chromatography (HPLC) procedure was utilized to isolate and purify $Sc_2S@C_{72}$.

Two synthetic methods have been employed for the production of dimetallic sulfide clusterfullerenes. Dunsch et al. introduced solid guanidium thiocyanate (CH_5N_3·HSCN) as the sulfur source and added it to the metal/graphite powder.[45] Using this method, a single isomer of $Sc_2S@C_{3v}(6)$-C_{82} was obtained as a minor product along with $Sc_3N@C_{80}$ and $Sc_3N@C_{78}$ as major products. Our method, using SO_2 as the sulfur source, gives SCFs as major products along with some OCFs as minor products. In our previous study we showed that an extensive family of $Sc_2S@C_{2n}$ (n = 40–50) could be obtained by this method.[46] In this study, as shown in Figure 1, SCFs with cages ranging from C_{68} to C_{80} were also obtained. This family, $Sc_2S@C_{2n}$ (n = 34–50), is unique in cage variety among all the clusterfullerene families. For both NCF and CCF families, cages

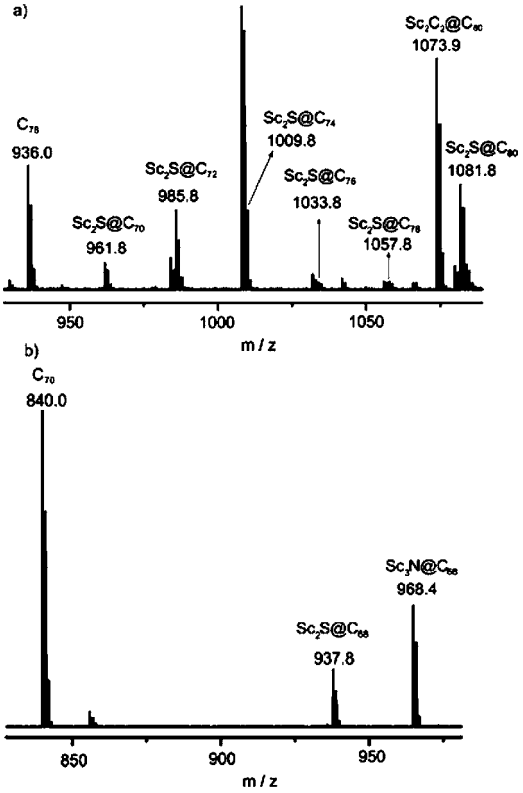

Figure 1. Mass spectra of (a) the raw extract of $Sc_2S@C_{2n}$ (n = 35–40) and (b) the isolated fraction containing $Sc_2S@C_{68}$.

C_{72} and C_{74} are still missing despite the fact that extensive work has been done in these areas for more than 10 years.[2]

$Sc_2S@C_{72}$ is the third smallest fullerene in the SCF family after $Sc_2S@C_{70}$ and $Sc_2S@C_{68}$ and was obtained in relatively high yield compared to the others. The HPLC–MALDI-TOF (MALDI-TOF = matrix-assisted laser desorption ionization time-of-flight) analysis shows that, on a 5PYE column, the $Sc_2S@C_{72}$ fraction overlaps with those of C_{76} and C_{78} (see Figure 2). This fraction was further separated by a two-stage recycling HPLC procedure running with a Buckyprep column and resulted in the isolation of pure $Sc_2S@C_{72}$ (see Figure S1 in the Supporting Information).

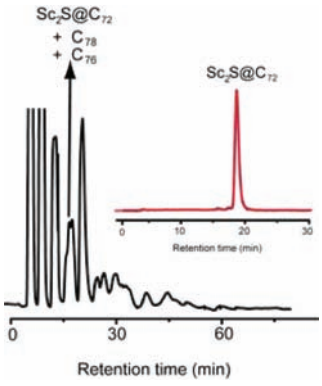

Figure 2. HPLC chromatograms of the fullerene extract obtained on a 10 mm × 250 mm 5PYE column with λ = 320 nm, a flow rate of 4 mL/min, and toluene as the eluant at 25 °C. Inset: HPLC-purified $Sc_2S@C_{72}$ obtained on a 10 mm × 250 mm Buckyprep column with λ = 320 nm, a flow rate of 4 mL/min, and toluene as the eluant at 25 °C.

dx.doi.org/10.1021/ja300765z | J. Am. Chem. Soc. 2012, 134, 7851–7860

The MALDI-TOF spectrum (Figure 3) of the isolated fraction shows a single peak at 985.973. The isotopic

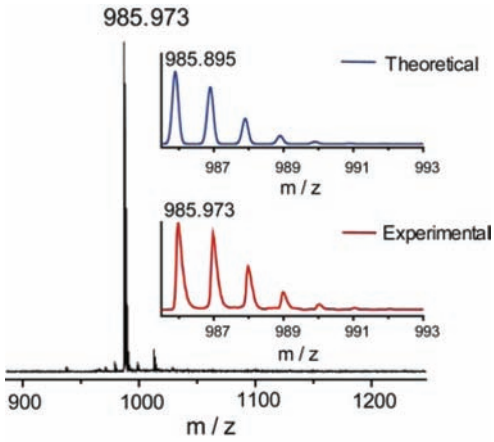

Figure 3. Mass spectrum of the purified $Sc_2S@C_{72}$. Inset: Experimental and theoretical isotopic distributions for $Sc_2S@C_{72}$.

distribution of the experimental MALDI spectrum was compared with the corresponding theoretical prediction and showed excellent agreement; see Figure 3. The purity of this sample was further checked by HPLC as shown in Figure 2.

The purified $Sc_2S@C_{72}$ has a yellow-green color in toluene solution. The UV−vis−NIR absorption of $Sc_2S@C_{72}$ is shown in Figure 4. A strong absorption occurs at 1076 nm with other

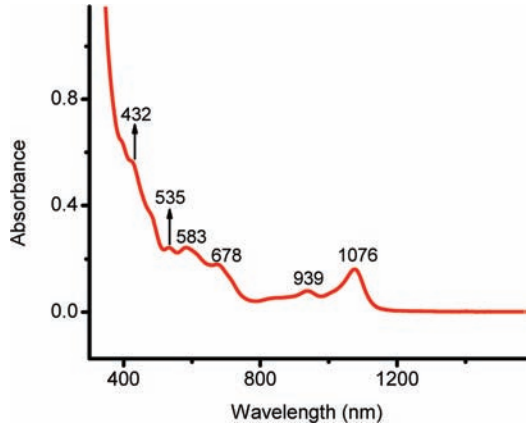

Figure 4. UV−vis−NIR absorption of $Sc_2S@C_{72}$ in CS_2 solution.

absorptions at 432, 535, 678, and 939 nm. The characteristic features of this spectrum are substantially different from those of $La@C_2$-C_{72},[10] $La_2@D_2(10611)$-C_{72},[55] and $C_{2v}(11188)$-$C_{72}Cl_4$.[53,54]

The absorption spectra of fullerenes in the visible and NIR are dominated by the $\pi-\pi^*$ transitions of the carbon cages, and the spectra are very sensitive to the carbon cage symmetries and electronic structures of the endohedral fullerenes as well.[5] Thus, the comparison of the UV−vis−NIR absorption is a convenient and diagnostic way to assign the cage symmetry of unknown endohedral fullerenes. The difference between the UV−vis−NIR spectrum of $Sc_2S@C_{72}$ and those of the other C_{72} isomeric cages reported thus far suggests that $Sc_2S@C_{72}$ has a different cage symmetry.

The band gap of this new isomer obtained from the spectral onset (1192 nm) is 1.04 eV. Using 1.0 eV as the limit to distinguish large- and small-band-gap fullerenes, we can assign $Sc_2S@C_{72}$ to a large-band-gap fullerene, and the gap is larger than those of the two isomers of $Sc_2S@C_{82}$.[46]

Crystallographic Studies. The crystal of $Sc_2S@C_s(10528)$-C_{72}·Ni^{II}(OEP)·1.5$CH_3C_6H_5$ (OEP = octaethylporphyrin) was obtained by slow diffusion of a toluene solution of Ni^{II}(OEP) into a toluene solution of the purified endohedral fullerene, followed by gradual evaporation until the sample was nearly dry. The crystal contains one ordered nickel octaethylporphyrin, an endohedral fullerene cage disordered over two orientations, a Sc_2S unit disordered over three sites, and an ordered and a disordered toluene molecule. A drawing of the major endohedral fullerene site and its orientation relative to the porphyrin is shown in Figure 5. The crystallographic data clearly show that a non-IPR cage is present and identify that cage as $C_s(10528)$-C_{72}, which is one of 11189 possible non-IPR isomers for C_{72}.

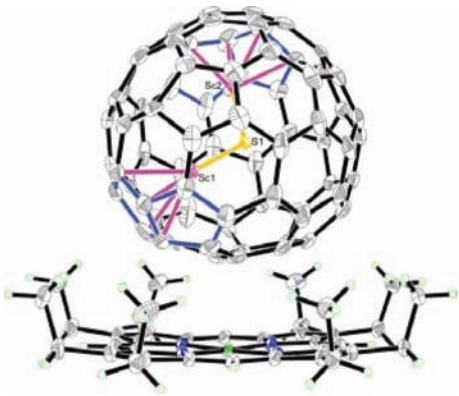

Figure 5. Thermal ellipsoid diagram, drawn at 40% probability, of the endohedral fullerene and the cocrystallized nickel octaethylporphyrin in $Sc_2S@C_{72}$·Ni^{II}(OEP)·1.5$CH_3C_6H_5$. Only the major cage orientation and Sc_2S unit are shown; solvate molecules have been omitted for clarity.

The fullerene cage and its contents are disordered. There are two orientations of the fullerene cage with refined occupancies of 0.50 each. The cage contents, Sc_2S, have been refined in three positions with occupancies of 0.503(13):0.379(13):0.116(12). The positions of S1, Sc1, and Sc2 are shown in Figure 5. The positions of S1′, Sc3, and Sc4 are similarly situated in the second cage orientation. In both of these situations, the scandium atoms reside near the pentalene sites where two pentagons of the fullerene cage abut. The shortest Sc−C distances involve the carbon atoms at the junctions of the two pentagons as seen in Table 1.

As seen in Figure 6, the C_{72} cage has C_s symmetry and two pentalene junctions shown in blue, which reside on opposite sides of the mirror plane. The ring spiral of this cage is **1 2** 9 11 13 16 24 27 29 **31** 34 **37**, with pentalene pentagons highlighted in bold. The endohedral moiety, the Sc_2S unit, has nearly C_{2v} symmetry, with similar lengths for the Sc−S bonds, which are given in Table 1. The scandium atom positions are nestled into the folds of the fused pentagons within their respective cages and display bonding that has become characteristic of non-IPR fullerenes. The cage, as viewed orthogonally to the Sc_2S unit, appears almost triangular, but when viewed parallel to the plane of the Sc_2S unit, the fullerene cage shows a typical roundness (see bottom view in Figure 6).

dx.doi.org/10.1021/ja300765z | J. Am. Chem. Soc. 2012, 134, 7851−7860

Table 1. Closest Sc−C and Sc−S Distances (Å) in $Sc_2S@C_s(10528)$-C_{72}[a]

Sc1		Sc2		Sc3		Sc4	
S1	2.325(3)	S1	2.347(3)	S1′	2.349(5)	S1′	2.353(5)
C1	2.257(4)	C49	2.240(10)	C1-2	2.206(5)	C65-2	2.238(4)
C2	2.287(7)	C65	2.241(4)	C5-2	2.240(7)	C49-2	2.268(6)
C5	2.300(5)	C64	2.269(6)	C2-2	2.265(5)	C64-2	2.282(5) Å
C8	2.311(5)	C66	2.314(5)	C8-2	2.279(6)	C66-2	2.301(5)
Sc1−S1−Sc2		125.36(14)°		Sc3−S1′−Sc4		123.8(2)°	

[a]The pentalene bonds are between C1 and C5 and C65 and C66.

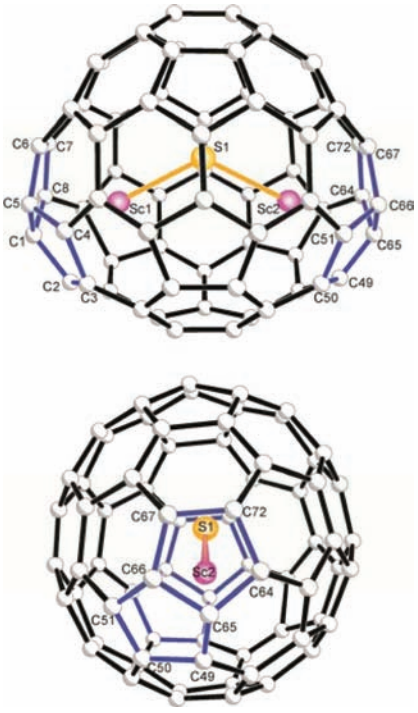

Figure 6. Two orthogonal views of one of the two orientations of $Sc_2S@C_s(10528)$-C_{72} showing the idealized mirror symmetry of the cage and contents.

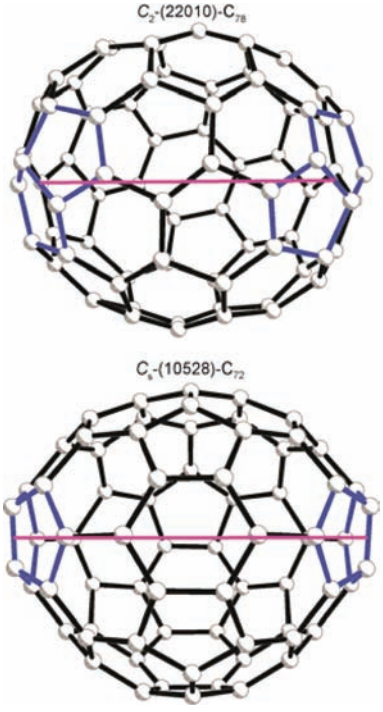

Figure 7. Comparison of the distances between pentalene centroids in $C_2(22010)$-C_{78} (top) and $C_s(10528)$-C_{72} (bottom). The distance between pentalene centroids is 6.83 Å for C_{78} versus 8.23 Å for C_{72}.

At the major site, the Sc_2S unit in $Sc_2S@C_s(10528)$-C_{72} has Sc−S bond distances that are nearly equivalent, 2.325(3) and 2.347(3) Å. These distances are just slightly shorter than the Sc−S bond distances in the two other structures with Sc_2S units: 2.335(3) and 2.416(4) Å in $Sc_2S@C_{3v}(8)$-C_{82} and 2.3525(8) and 2.3902(8) Å in $Sc_2S@C_s(6)$-C_{82}.[47] However, the Sc1−S1−Sc2 angle in $Sc_2S@C_s(10528)$-C_{72} (125.36(14)°) is noticeably more obtuse than the corresponding angles in $Sc_2S@C_{3v}(8)$-C_{82} (97.34(13)°) and $Sc_2S@C_s(6)$-C_{82} (113.84(3)°).[47] The fact the Sc1−S1−Sc2 angle in the small C_{72} cage is actually larger than the corresponding angles in the larger C_{82} cages might be rationalized by the stronger interaction between the scandium atoms and their corresponding pentalene units and the location of these units in the C_{72} cage.

An interesting comparison can be made between the $Sc_2S@C_s(10528)$-C_{72} and the only other pristine endohedral with two pentalene units, $Gd_3N@C_2(22010)$-C_{78}. Despite the larger C_{78} cage and the more ponderous Gd_3N unit, the separation between the pentalenes is greater in $Sc_2S@C_s(10528)$-C_{72} than in $Gd_3N@C_2(22010)$-C_{78}.[12] This feature is shown in Figure 7. This greater separation between the pentalene motifs is interesting, but not entirely unexpected, since the Sc−S distances are larger than the Gd−N distances and the Sc−S−Sc angle is wider than the Gd−N−Gd angle.

The approach of the fullerene cage to the porphyrin is fairly typical, with close distances of 2.813(5) and 2.793(6) Å from the nickel atom to the nearest carbon atoms in the first and second cage orientations, respectively. The packing is also typical of cocrystallized fullerenes and porphyrins. Each fullerene cage is embraced by the eight ethyl arms of a porphyrin. The porphyrins are stacked back to back, and the fullerene cage packs among other fullerenes and solvent molecules using $\pi-\pi$ interactions. The fullerene−fullerene interactions are shorter than the distance between the planes in graphite (3.35 Å), with the shortest being 2.82(3) Å, but most of them are in the range of 2.9−3.0 Å. These interactions are also shorter than those that have been observed in the crystal structure of $Sc_2S@C_s(6)$-C_{82}.

Computational Studies. The structure for $Sc_2S@C_s(10528)$-C_{72} was optimized at the DFT BP86/TZP level. Structural parameters very similar to those observed for the experimental X-ray structure were found (for example, 2.345 Å for the Sc−S distance and 124.4° for the Sc−S−Sc angle, to be

dx.doi.org/10.1021/ja300765z | J. Am. Chem. Soc. 2012, 134, 7851−7860

compared with the values found from X-ray crystallography, 2.344 Å and 124. 6°, respectively); see Figure 8.

Figure 8. DFT-optimized structure for $Sc_2S@C_s(10528)\text{-}C_{72}$.

From the electronic structure of $Sc_2S@C_{72}(10528)$, we have verified that a formal transfer of four electrons from the Sc_2S cluster to the C_{72} cage occurs, i.e., $(Sc_2S)^{4+}@(C_{72})^{4-}$, as depicted in the orbital interaction diagram in Figure 9, which

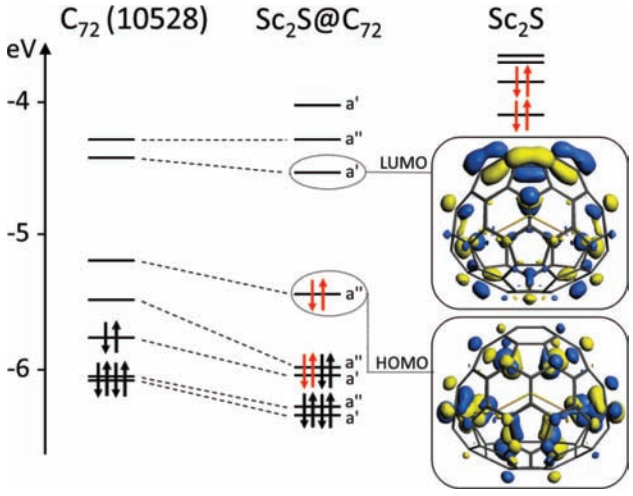

Figure 9. Orbital interaction diagram for $Sc_2S@C_s(10528)\text{-}C_{72}$. The fragments Sc_2S and $C_s(10528)\text{-}C_{72}$ are calculated with the geometry that they have in the endohedral fullerene.

shows that the HOMO and LUMO are mainly localized on the C_{72} framework. Therefore, the electronic structure of all the EMFs (endohedral metallic fullerenes) that contain clusters of the type Sc_2X known so far, with X = S or O, can be easily explained taking into consideration an ionic model with a formal transfer of four electrons from the cluster to the cage.[44,47]

To predict the stability of a given clusterfullerene, however, one also has to take into consideration that significant interactions between the metal atoms of the cluster and specific structural motifs on the carbon cage may exist. For IPR clusterfullerenes with sufficiently large cages, for example, $M_3N@C_{2n}$ ($2n > 78$), $Sc_4O_k@I_h\text{-}C_{80}$ ($k = 2, 3$), $Sc_2X@C_{82}$ (X = S, O), and $M_2C_2@C_{2n}$ ($2n = 82, 84$), where the metal cluster has enough space to rotate, the M···cage interactions are not as critical as in the clusterfullernes that show one or more adjacent pentagon pairs (APPs). It is seen that clusterfullerenes with non-IPR cages are stabilized when the metal atoms of the cluster point to the APPs, as in $Sc_3N@D_3(6140)\text{-}C_{68}$,[13] $Gd_3N@C_s(39663)\text{-}C_{82}$,[49] $M_3N@C_s(51365)\text{-}C_{84}$,[15] and now in $Sc_2S@C_s(10528)\text{-}C_{72}$. Therefore, proper positioning of the pentalene motifs within the non-IPR cage that allows an optimized interaction with the metal cluster is crucial to stabilize non-IPR EMFs. For the present case, isomer 10528 is not only the most favored tetraanionic cage, but also the cage with the most favored disposition of the two pentalene units to interact with the two Sc atoms of the internal cluster (see Figures 8 and 10).

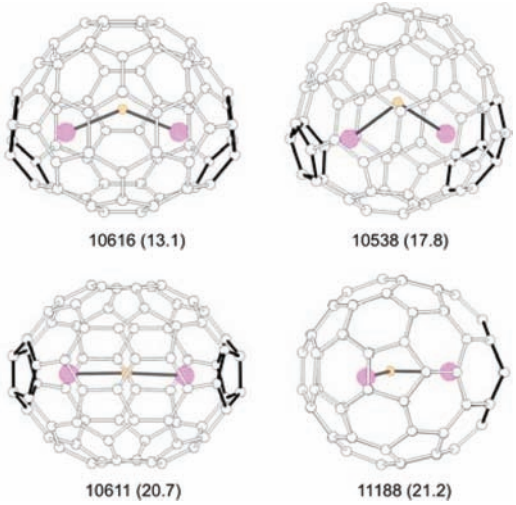

Figure 10. Optimized structures for different cage isomers of $Sc_2S@C_{72}$ with their relative energies, kcal mol^{-1}, in parentheses with respect to the lowest energy $Sc_2S@C_s(10528)\text{-}C_{72}$ isomer.

Cage 10611, which also has a low number of pyracylene motifs and a small value of the IPSI (inverse pentagon separation index), similar to cage 10528,[49] is energetically comparable to cage 10528 in the tetraanionic state (only 1.7 kcal mol^{-1} higher in energy, third column of Table 2). It is important to note that

Table 2. Relative Energies, kcal mol^{-1}, for the Lowest Energy Isomers of C_{72}^{4-} and $Sc_2S@C_{72}$, along with Their Number of APPs, Number of Pyracylenes, and IPSI Values, Å^{-1}, in the Tetraanionic Cages

isomer	no. of APPs	C_{72}^{4-}	$Sc_2S@C_{72}$	no. of pyracylenes	IPSI
10528	2	0.0	0.0	8	13.4996
10611	2	1.7	20.7	6	13.4986
10616	2	4.5	13.1	8	13.5041
11188	1	6.5	21.2	14	13.3922
10610	2	8.8	22.4	9	13.5034
10538	2	14.8	17.8	11	13.5078
10626	2	15.2	28.3	10	13.5097
10612	1	15.2	28.3	15	13.3926

cage 10611 leads to a much more destabilized clusterfullerene (around 20 kcal mol^{-1}) because the Sc_2S is forced to be in an almost linear arrangement (Sc−S−Sc angle 171.4°) due to the location of the two pentalene motifs (see Figure 10). A similar destabilization occurs for isomer 10626, which is 15 kcal mol^{-1} higher in energy than $C_s(10528)\text{-}C_{72}^{4-}$. The second lowest energy EMF is $Sc_2S@C_s(10616)\text{-}C_{72}$, with a relative energy of 13 kcal mol^{-1}, and with the cluster slightly distorted (Sc−S−Sc angle 134.1°) compared to that of $Sc_2S@C_s(10528)\text{-}C_{72}$. It is also worth mentioning that the $Sc_2S@C_{72}$ isomers with only one APP are also destabilized by more than 20 kcal mol^{-1} due

dx.doi.org/10.1021/ja300765z | J. Am. Chem. Soc. 2012, 134, 7851−7860

Table 3. Experimental and TDDFT Predictions for the Most Intense Low-Energy Excitations in the Absorption Spectrum of $Sc_2S@C_s(10528)$-C_{72}

exptl λ (nm)	exptl E (eV)	excited state	calcd E (eV)	f^a	leading configurations[b] (%)
1076	1.15	S_1-$1^1A''$	1.14	0.00994	HOMO → LUMO (98)
939	1.32	S_2-$1^1A'$	1.34	0.00261	HOMO → LUMO + 1 (96)
		S_5-$2^1A'$	1.68	0.01366	HOMO − 2 → LUMO (88)
678	1.83	S_7-$5^1A''$	1.82	0.00630	HOMO − 3 → LUMO (50), HOMO → LUMO + 3 (41)
		S_8-$3^1A'$	1.83	0.00987	HOMO − 1 → LUMO + 1 (91)
		S_9-$6^1A''$	1.84	0.00201	HOMO − 2 → LUMO + 1 (82), HOMO → LUMO + 3 (14)
583	2.13	S_{15}-$9^1A''$	2.11	0.00121	HOMO − 4 → LUMO + 1 (59), HOMO − 5 → LUMO + 1 (35)
		S_{16}-$7^1A'$	2.12	0.00484	HOMO − 2 → LUMO + 2 (90)
		S_{18}-$10^1A''$	2.15	0.00305	HOMO − 5 → LUMO + 1 (61), HOMO − 4 → LUMO + 1 (24)
535	2.32	S_{21}-$12^1A''$	2.29	0.00306	HOMO − 1 → LUMO + 3 (63), HOMO → LUMO + 7 (14), HOMO − 7 → LUMO (12)
		S_{25}-$11^1A'$	2.37	0.00242	HOMO − 2 → LUMO + 3 (78), HOMO − 2 → LUMO + 4 (12)
		S_{26}-$15^1A''$	2.38	0.00797	HOMO − 8 → LUMO (30), HOMO → LUMO + 8 (24)

[a]Only excitations with f (oscillator strength) > 0.001 are listed. [b]Contributions of less than 10% are omitted.

to the fact that only one favorable Sc···pentalene interaction exists. Therefore, isomer 10528 is the most favorable cage to encapsulate the Sc_2S cluster because (i) it is the most favored tetraanion and (ii) it has the proper location of the pentalene motifs to optimize the interaction with the metal cluster.

Besides the analysis of the electronic structure and the relative stability of the different isomers of $Sc_2S@C_{72}$, the computational study of the UV−vis−NIR absorption spectrum of $Sc_2S@C_s(10528)$-C_{72} has also been performed by means of time-dependent (TD) DFT calculations (see Table 3 and Figure S4, Supporting Information). Despite the systematic underestimation of excitation energies by TDDFT, this methodology provides a reasonable agreement with experiments and allows the assignment of absorption bands to electronic transitions within the molecule. In the present case, the strong NIR absorption at 1076 nm (1.15 eV) is assigned to the HOMO → LUMO excitation with a predicted energy of 1.14 eV. The much weaker peak at 939 nm (1.32 eV) is assigned to the HOMO → LUMO + 1 transition (predicted at 1.34 eV). The assignment of other highlighted peaks of the absorption spectrum in Figure 4 is detailed in Table 3.

^{45}Sc NMR Studies. A single line at 183.3 ppm was found in the ^{45}Sc NMR spectrum of $Sc_2S@C_s(10528)$-C_{72}, which is more strongly shielded than the corresponding ^{45}Sc NMR signal for $Sc_2S@C_{3v}(8)$-C_{82} at 290 ppm.[45] This result shows that the cage size and structure have a dramatic effect on the chemical shift of the ^{45}Sc NMR spectrum. A similar sensitivity of the ^{89}Y NMR chemical shift to the change of cage structures was also observed in the study of a series of yttrium NCF compounds, in which the ^{89}Y NMR signals were observed at 191.63 and 62.65 ppm for $Y_3N@I_h(8)$-C_{80} and $Y_3N@D_3(19)$-C_{86}, respectively.[60] Furthermore, the single ^{45}Sc signal suggests that either the two Sc ions are equivalent or fast cluster rotation averaged the signal of the cluster. In the study of $Y_3N@C_s(51365)$-C_{84}, a non-IPR NCF, three ^{89}Y NMR signals were observed, suggesting that the rotation of the Y_3N cluster was hindered by the coordination between Y^{3+} ions and the pentalene motifs.[60] In our study, as the crystallographic studies of $Sc_2S@C_s(10528)$-C_{72} point out, the coordination between the Sc^{3+} ions and the vicinal pentalene motifs also exists, which is characteristic for non-IPR CFs. Furthermore, all the computational attempts to optimize the geometry of the clusterfullerene with different orientations of the Sc_2S unit lead to the same result, i.e., the orientation observed in the X-ray structure. Thus, it is more likely that two equivalent Sc ions exist in the rotationally hindered Sc_2S cluster, rather than fast rotation of the Sc_2S cluster, giving rise to the single ^{45}Sc NMR signal.

Electrochemical Studies. The cyclic voltammograms (CVs) of $Sc_2S@C_s(10528)$-C_{72} were recorded in *o*-dichlorobenzene (*o*-DCB) containing 0.05 M tetra-*n*-butylammonium hexafluorophosphate (*n*-Bu_4NPF_6) as the supporting electrolyte using a scan rate of 100 mV s^{-1} (Figure 11).

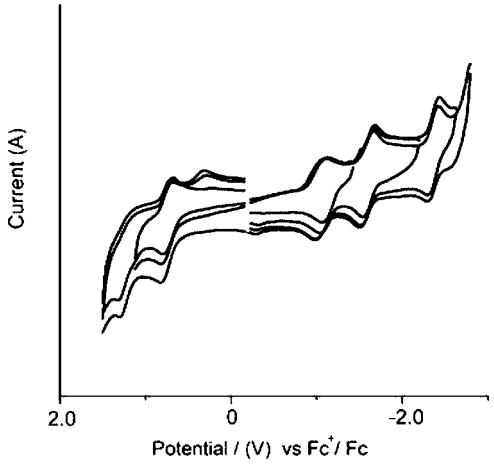

Figure 11. Cyclic voltammograms of $Sc_2S@C_s(10528)$-C_{72} in *n*-Bu_4NPF_6/*o*-DCB with ferrocene as the internal standard (scan rate 100 mV s^{-1}).

The CV of $Sc_2S@C_s(10528)$-C_{72} shows major differences from those of the other metallic sulfide fullerenes, $Sc_2S@C_{3v}(8)$-C_{82} and $Sc_2S@C_s(6)$-C_{82}, both for oxidation and reduction processes.[46] On the reductive scan, the CVs of the two isomers of $Sc_2S@C_{82}$ show irreversible or quasi-reversible reduction steps. However, the reduction steps for $Sc_2S@C_s(10528)$-C_{72} are reversible, a rather uncommon observation for metallic CFs. This difference shows that the cage structure has a significant effect on the electrochemical behavior of the fullerenes. Interestingly, this reversible reductive behavior is very similar to that of $TiSc_2N@C_{80}$, a mixed metal NCF, another rare sample of CF demonstrating reversible reduction steps, while the reductions of other homometallic NCFs are electrochemically irreversible under the same conditions.[36,61,62]

dx.doi.org/10.1021/ja300765z | J. Am. Chem. Soc. 2012, 134, 7851−7860

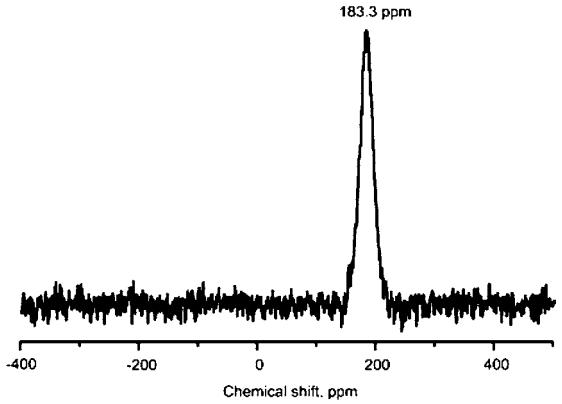

Figure 12. ^{45}Sc NMR spectrum of $Sc_2S@C_s(10528)$-C_{72}.

The similarities between the reductive behavior of these two CFs show that changes of the cluster structures also play an important role in the reductive behavior. Thus, the unique reductive behavior of $Sc_2S@C_s(10528)$-C_{72} is the result of a combined effect of both the cage structure and the encaged cluster.

On the other hand, while most of the metallic clusterfullerenes, including the two isomers of $Sc_2S@C_{82}$, show a reversible oxidative process, the CV of $Sc_2S@C_s(10528)$-C_{72} shows a reversible first oxidation followed by an irreversible second oxidation step.[63] As Figure 11 shows, if the potential is swept only to the first oxidation step, the corresponding reduction step is reversible. However, if the potential is swept to the second oxidation step, in addition to the two re-reduction steps, a third one appears before the corresponding reduction step of the first oxidation step. This oxidative behavior suggests that the monocation of $Sc_2S@C_s(10528)$-C_{72} is stable but the dication is unstable and the second oxidation step is followed by a fast structural rearrangement which gives rise to the third re-reduction step. Similar electrochemical behavior has been observed in the study of other NCFs.[63,64] Because the electrochemical oxidation is chemically reversible as no significant change in the oxidation steps were observed during the multiple redox cycles, the follow-up reaction could be attributed either to intermolecular rearrangement or to a reaction between the dications.[62,64]

The redox potentials of $Sc_2S@C_s(10528)$-C_{72} also show significant differences from those of the two isomers of $Sc_2S@C_{82}$ (Table 4). The reduction potentials are dramatically more negative than those of the two isomers of $Sc_2S@C_{82}$, suggesting a much weaker electron-accepting ability. On the other hand, the first oxidation potential of $Sc_2S@C_s(10528)$-C_{72} is also much higher than those of the two isomers of $Sc_2S@C_{82}$, shifting from +0.52 V for $Sc_2S@C_{3v}(8)$-C_{82} and +0.39 V for $Sc_2S@C_s(6)$-C_{82} to +0.64 V for $Sc_2S@C_s(10528)$-C_{72}, indicating a higher ionization potential. Thus, the electrochemical gap of $Sc_2S@C_s(10528)$-C_{72} is 1.78 eV, substantially larger than those of the corresponding $Sc_2S@C_{82}$ isomers (1.56 eV for $Sc_2S@C_{3v}(8)$-C_{82} and 1.47 eV for $Sc_2S@C_s(6)$-C_{82}).

DISCUSSION

$Sc_2S@C_s(10528)$-C_{72} is the first non-IPR SCF isolated to date. $Sc_2S@C_s(10528)$-C_{72} also represents a fourth cage isomer of C_{72}, all four being non-IPR isomers. Since these non-IPR fullerenes possess different encaged species, they give a rare chance to examine how the different encaged species affect the choice of one particular cage out of the 11189 possible non-IPR isomers for C_{72}.[10,53,54,57]

In the stabilization of clusterfullerenes, the important role of charge transfer from the cluster to the cage has been widely acknowledged. This is verified again in the case of $Sc_2S@C_s(10528)$-C_{72} as $C_s(10528)$-C_{72}^{4-} has been identified as the most stable tetraanion among all the C_{72} cage isomers. However, the computational study also suggests that $D_2(10611)$-C_{72} and $C_s(10528)$-C_{72} have similar stabilities in their tetraanionic and hexaanionic forms. $C_s(10528)$-C_{72}^{6-} is 13.6 kcal mol^{-1} less stable than $D_2(10611)$-C_{72}^{6-}, while $D_2(10611)$-C_{72}^{4-} is only 1.7 kcal mol^{-1} higher in energy than $C_s(10528)$-C_{72}^{4-}.

$La_2@C_{72}$ was isolated and characterized as $La_2@C_{72}$(2-adamantane-2,3-[3*H*]-diaziridine) and shown to have $D_2(10611)$-C_{72} symmetry, which is in agreement with theoretical calculations that indicate that $D_2(10611)$-C_{72}^{6-} is the most stable hexaanion for the C_{72} cage.[55] $Sc_3N@C_{72}$ has an electronic structure similar to that of $La_2@C_{72}$, since these clusters transfer six electrons to the C_{72} cage.[58] This molecule was proposed to have a $C_s(10528)$-C_{72} cage symmetry.[58] However, no endohedral with the composition $M_3N@C_{72}$ has been experimentally detected. This situation shows that, besides the charge transfer, the properties of the encaged species also play a major role in the selection of the cage symmetry.

For $La_2@C_{72}$, the two La ions are free to move around inside the cage as there is no direct bonding between them. On the other hand, these two La ions must stay away from each other because of the strong repulsion between them.[55] $D_2(10611)$-C_{72} has both favorable energies and structural complementarity, since the two APPs are at the pole regions of the cage C_{72}, thus facilitating maxium separation of the trapped ions. The crystallographic results show that the two La atoms reside at the two poles of C_{72}.[55] With the La−La axis perpendicular to the two [5,5] bonds, this structural arrangement not only favors the strong interaction between the caged metal ions and the [5,5] junctions, which are essential for stabilization, but also keeps the two La ions far away from each other.

For $Sc_3N@D_2(10611)$-C_{72}, however, the Sc_3N unit would have to be highly distorted to coordinate the two APPs because they are located at the poles of the fullerene.[58] Even for the most stable $C_s(10528)$-C_{72} cage, the Sc_3N cluster would have to

Table 4. Redox Potentials of $Sc_2S@C_s(10528)$-C_{72}, $Sc_2S@C_s(6)$-C_{82}, and $Sc_2S@C_{3v}(8)$-C_{82} in *n*-Bu_4NPF_6/*o*-DCB with Ferrocene as the Internal Standard (Scan Rate 100 mV s^{-1})

compound	$E^{1+/2+}$	$E^{0/+}$	$E^{0/-}$	$E^{1-/2-}$	$E^{2-/3-}$
$Sc_2S@C_s(10528)$-C_{72}	+1.21[b]	+0.64[a] (110)	−1.14[a] (140)	−1.53[a] (140)	−2.24[a] (117)
$Sc_2S@C_s(6)$-C_{82}	+0.65[b]	+0.39[a] (88)	−0.98[b]	−1.12[a] (121)	−1.73[a] (129)
$Sc_2S@C_{3v}(8)$-C_{82}	+0.96[b]	+0.52[b]	−1.04[b]	−1.19[b]	−1.63[b]

[a]Half-wave potentials. The values in parentheses are the differences between the peak potentials and the half-wave potentials in millivolts. Scan rate 100 mV s^{-1}. [b]Peak potentials.

dx.doi.org/10.1021/ja300765z | *J. Am. Chem. Soc.* 2012, 134, 7851−7860

be distorted severely from a planar trigonal structure to coordinate with the two APPs. Thus, the mismatch between the shape of the Sc_3N unit and the location of the APPs of the C_{72} cage becomes a major obstacle to the stabilization of this cage.

Compared to the Sc_3N cluster, the geometry of the Sc_2S unit makes it easier to coordinate the two scandium ions to the two APPs on $C_s(10528)$-C_{72} and avoids severe distortion, which is inevitable for any M_3N cluster. The crystallographic analysis shows that the Sc_2S cluster is tilted and then puts the scandium atoms closer to one end of the pentalene bond. Thus, the geometry effect of the Sc_2S cluster, together with the four-electron charge transfer from the Sc_2S cluster to the cage, stabilizes $C_s(10528)$-C_{72}, which has never been obtained from any other clusterfullerene family reported to date.

CONCLUSION

A non-IPR metallic sulfide clusterfullerene, $Sc_2S@C_s(10528)$-C_{72}, has been isolated and characterized by mass spectrometry, UV−vis−NIR absorption spectroscopy, cyclic voltammetry, ^{45}Sc NMR, and single-crystal X-ray diffraction. The single-crystal diffraction study clearly shows that the C_{72} fullerene cage does not follow the IPR rule, and the cage symmetry was assigned to $C_s(10528)$-C_{72}. The electrochemical behavior of $Sc_2S@C_s(10528)$-C_{72} demonstrates a major difference from those of the $Sc_2S@C_s$-C_{82} as well as the other metallic clusterfullerenes. Computational studies show that the Sc_2S cluster transfers four electrons to the C_{72} cage and C_s-$C_{72}(10528)$ is the most stable cage for both empty C_{72}^{4-} and $Sc_2S@C_{72}$. The structural differences between the reported fullerenes with C_{72} cages indicate that the shape and properties of the encaged clusters play an important role in the selection of the parent non-IPR cages. $Sc_2S@C_s(10528)$-C_{72} is the first example for which the combined effect of a four-electron transfer and the special geometry of the Sc_2S cluster help to stabilize a new carbon cage that is not observed for other clusterfullerene families.

EXPERIMENTAL SECTION

X-ray Crystallography and Data Collection for $Sc_2S@C_s(10528)$-C_{72}·Ni^{II}(OEP)·1.5(toluene). $C_{118.50}H_{56}N_4NiSSc_2$, M = 1716.36, black parallelepiped, 0.08 mm × 0.07 mm × 0.03 mm, Advanced Light Source, beamline 11.3.1, triclinic, space group $P\bar{1}$ (No. 2), a = 15.1733(4) Å, b = 15.9533(4) Å, c = 16.7953(4) Å, α = 76.032(2)°, β = 74.752(2)°, γ = 65.310(2)°, λ = 0.77490 Å, T = 100(2) K, V = 3523.50(15) Å^3, Z = 2, 163 650 reflections measured, 33 273 unique reflections (R_{int} = 0.0510) that were used in all calculations, Bruker SMART Apex II, $2\theta_{max}$ = 80.62°, min/max transmission 0.6086/0.9796 (multiscan absorption correction applied, TWINABS), direct methods and difference Fourier methods solution, full-matrix least-squares based on F^2 (SHELXS97 and SHELXL97), final wR2(F^2) = 0.1625 (all data), conventional R1 = 0.0569 computed for 1837 parameters with 84 restraints.

Computational Details. The calculations were carried out using DFT methodology with the ADF 2010 program.[65,66] The exchange-correlation functionals of Becke[67] and Perdew[68] were used. Relativistic corrections were included by means of the ZORA formalism. Slater triple-ζ + polarization basis sets were employed to describe the valence electrons of C, S, and Sc. Frozen cores consisting of the 1s shell for C and the 1s to 2p shells for S and Sc were described by means of single Slater functions.

^{45}Sc NMR. The ^{45}Sc NMR spectroscopic measurements were performed at 145 MHz in a PFG, NM-60TH5AT/FG probe of a JEOL ECA 600 spectrometer at room temperature in carbon disulfide solutions with d_3-toluene as the lock and a 0.2 M $Sc(NO_3)_3$ solution in concentrated HNO_3 as the reference.

Electrochemistry. Cyclic voltammetry experiments were performed on a BAS 100B workstation at room temperature under the protection of argon gas flow. A 1 mm diameter glassy carbon was used as the working electrode, and platinum wire and silver wire were employed as the counter electrode and reference electrode, respectively. The supporting electrolyte tetra-*n*-butylammonium hexafluorophosphate, *n*-Bu_4NPF_6 (electrochemical grade, Sigma Aldrich), was dried under reduced pressure at 340 K for 24 h and stored in a glovebox prior to use. The concentration of *n*-Bu_4NPF_6 in *o*-DCB solutions was 0.05 mol/L. Ferrocene (Fc) was added as the internal standard for final voltammetric cycle, and all potentials are referred to the Fc/Fc^+ couple.

ASSOCIATED CONTENT

Supporting Information

HPLC separation details, computational details and results, and X-ray crystallographic files in CIF format for $Sc_2S@C_s(10528)$-C_{72}·Ni^{II}(OEP)·1.5(toluene). This material is available free of charge via the Internet at http://pubs.acs.org.

AUTHOR INFORMATION

Corresponding Author

mmolmstead@ucdavis.edu; albalch@ucdavis.edu; josepmaria.poblet@urv.cat; echegoyen@utep.edu

Notes

The authors declare no competing financial interest.

ACKNOWLEDGMENTS

L.E. thanks the Robert A. Welch Foundation for an endowed chair, Grant AH-0033, and the U.S. National Science Foundation (NSF) for Grant CHE-1110967, which provided generous support for this work. A.L.B. and M.M.O. thank the U.S. NSF (Grant CHE-1011760) for support of this work and Dr. Simon Teat and The Advanced Light Source, supported by the Director, Office of Science, Office of Basic Energy Sciences, of the U.S. Department of Energy under Contract DE-AC02-05CH11231, for beam time. This work is also supported by the Spanish Ministry of Science and Innovation (Project CTQ2011-29054-C02-01) and by the Generalitat de Catalunya (Grants 2009SGR462 and XRQTC).

REFERENCES

(1) Chen, N.; Ortiz, A. L.; Echegoyen, L. *Fullerenes: Principles and Applications*, 2nd ed.; The Royal Society of Chemistry: London, 2012; p 12.
(2) Yang, S.; Liu, F.; Chen, C.; Jiao, M.; Wei, T. *Chem. Commun.* **2011**, *47*, 11822.
(3) Dunsch, L.; Yang, S. *Phys. Chem. Chem. Phys.* **2007**, *9*, 3067.
(4) Dunsch, L.; Yang, S. *Small* **2007**, *3*, 1298.
(5) Shinohara, H. *Rep. Prog. Phys.* **2000**, *63*, 843.
(6) Murata, Y.; Murata, M.; Komatsu, K. *J. Am. Chem. Soc.* **2003**, *125*, 7152.
(7) Martin, N. *Chem. Commun.* **2006**, 2093.
(8) Wang, C. R.; Kai, T.; Tomiyama, T.; Yoshida, T.; Kobayashi, Y.; Nishibori, E.; Takata, M.; Sakata, M.; Shinohara, H. *Nature* **2000**, *408*, 426.
(9) Kato, H.; Taninaka, A.; Sugai, T.; Shinohara, H. *J. Am. Chem. Soc.* **2003**, *125*, 7782.
(10) Wakahara, T.; Nikawa, H.; Kikuchi, T.; Nakahodo, T.; Rahman, G. M. A.; Tsuchiya, T.; Maeda, Y.; Akasaka, T.; Yoza, K.; Horn, E.; Yamamoto, K.; Mizorogi, N.; Slanina, Z.; Nagase, S. *J. Am. Chem. Soc.* **2006**, *128*, 14228.
(11) Wang, T. S.; Feng, L.; Wu, J. Y.; Xu, W.; Xiang, J. F.; Tan, K.; Ma, Y. H.; Zheng, J. P.; Jiang, L.; Lu, X.; Shu, C. Y.; Wang, C. R. *J. Am. Chem. Soc.* **2010**, *132*, 16362.

(12) Beavers, C. M.; Chaur, M. N.; Olmstead, M. M.; Echegoyen, L.; Balch, A. L. *J. Am. Chem. Soc.* **2009**, *131*, 11519.
(13) Stevenson, S.; Fowler, P. W.; Heine, T.; Duchamp, J. C.; Rice, G.; Glass, T.; Harich, K.; Hajdu, E.; Bible, R.; Dorn, H. C. *Nature* **2000**, *408*, 427.
(14) Yang, S. F.; Popov, A. A.; Dunsch, L. *Angew. Chem., Int. Ed.* **2007**, *46*, 1256.
(15) Zuo, T.; Walker, K.; Olmstead, M. M.; Melin, F.; Holloway, B. C.; Echegoyen, L.; Dorn, H. C.; Chaur, M. N.; Chancellor, C. J.; Beavers, C. M.; Balch, A. L.; Athans, A. J. *Chem. Commun.* **2008**, 1067.
(16) Feng, M.; Zhao, J.; Huang, T.; Zhu, X.; Petek, H. *Acc. Chem. Res.* **2011**, *44*, 360.
(17) Akasaka, T.; Nagase, S. *Endofullerenes: A New Family of Carbon Clusters*; Kluwer Academic Publishers: Dordrecht, The Netherlands, Boston, MA, 2002.
(18) Mikawa, M.; Kato, H.; Okumura, M.; Narazaki, M.; Kanazawa, Y.; Miwa, N.; Shinohara, H. *Bioconjugate Chem.* **2001**, *12*, 510.
(19) Bolskar, R. D.; Benedetto, A. F.; Husebo, L. O.; Price, R. E.; Jackson, E. F.; Wallace, S.; Wilson, L. J.; Alford, J. M. *J. Am. Chem. Soc.* **2003**, *125*, 5471.
(20) Kato, H.; Kanazawa, Y.; Okumura, M.; Taninaka, A.; Yokawa, T.; Shinohara, H. *J. Am. Chem. Soc.* **2003**, *125*, 4391.
(21) Shu, C.-Y.; Gan, L.-H.; Wang, C.-R.; Pei, X.-l.; Han, H.-b. *Carbon* **2006**, *44*, 496.
(22) Ross, R. B.; Cardona, C. M.; Guldi, D. M.; Sankaranarayanan, S. G.; Reese, M. O.; Kopidakis, N.; Peet, J.; Walker, B.; Bazan, G. C.; Van Keuren, E.; Holloway, B. C.; Drees, M. *Nat. Mater.* **2009**, *8*, 208.
(23) Pinzón, J. R.; Cardona, C. M.; Herranz, M. Á.; Plonska-Brzezinska, M. E.; Palkar, A.; Athans, A. J.; Martín, N.; Rodríguez-Fortea, A.; Poblet, J. M.; Bottari, G.; Torres, T.; Gayathri, S. S.; Guldi, D. M.; Echegoyen, L. *Chem.—Eur. J.* **2009**, *15*, 864.
(24) Ross, R. B.; Cardona, C. M.; Swain, F. B.; Guldi, D. M.; Sankaranarayanan, S. G.; Keuren, E. V.; Holloway, B. C.; Drees, M. *Adv. Funct. Mater.* **2009**, *19*, 2332.
(25) Pinzón, J. R.; Plonska-Brzezinska, M. E.; Cardona, C. M.; Athans, A. J.; Gayathri, S. S.; Guldi, D. M.; Herranz, M. A.; Martin, N.; Torres, T.; Echegoyen, L. *Angew. Chem., Int. Ed.* **2008**, *47*, 4173.
(26) Feng, L.; Gayathri Radhakrishnan, S.; Mizorogi, N.; Slanina, Z.; Nikawa, H.; Tsuchiya, T.; Akasaka, T.; Nagase, S.; Martín, N.; Guldi, D. M. *J. Am. Chem. Soc.* **2011**, *133*, 7608.
(27) Yamada, M.; Akasaka, T.; Nagase, S. *Acc. Chem. Res.* **2010**, *43*, 92.
(28) Hajjaj, F.; Tashiro, K.; Nikawa, H.; Mizorogi, N.; Akasaka, T.; Nagase, S.; Furukawa, K.; Kato, T.; Aida, T. *J. Am. Chem. Soc.* **2011**, *113*, 9290.
(29) Stevenson, S.; Rice, G.; Glass, T.; Harich, K.; Cromer, F.; Jordan, M. R.; Craft, J.; Hadju, E.; Bible, R.; Olmstead, M. M.; Maitra, K.; Fisher, A. J.; Balch, A. L.; Dorn, H. C. *Nature* **1999**, *401*, 55.
(30) Yang, H.; Jin, H.; Zhen, H.; Wang, Z.; Liu, Z.; Beavers, C. M.; Mercado, B. Q.; Olmstead, M. M.; Balch, A. L. *J. Am. Chem. Soc.* **2011**, *133*, 6299.
(31) Mercado, B. Q.; Jiang, A.; Yang, H.; Wang, Z.; Jin, H.; Liu, Z.; Olmstead, M. M.; Balch, A. L. *Angew. Chem., Int. Ed.* **2009**, *48*, 9114.
(32) Che, Y.; Yang, H.; Wang, Z.; Jin, H.; Liu, Z.; Lu, C.; Zuo, T.; Dorn, H. C.; Beavers, C. M.; Olmstead, M. M.; Balch, A. L. *Inorg. Chem.* **2009**, *48*, 6004.
(33) Chaur, M. N.; Melin, F.; Elliott, B.; Kumbhar, A.; Athans, A. J.; Echegoyen, L. *Chem.—Eur. J.* **2008**, *14*, 4594.
(34) Chaur, M. N.; Melin, F.; Ashby, J.; Elliott, B.; Kumbhar, A.; Rao, A. M.; Echegoyen, L. *Chem.—Eur. J.* **2008**, *14*, 8213.
(35) Stevenson, S.; Ling, Y.; Coumbe, C. E.; Mackey, M. A.; Confait, B. S.; Phillips, J. P.; Dorn, H. C.; Zhang, Y. *J. Am. Chem. Soc.* **2009**, *131*, 17780.
(36) Yang, S. F.; Chen, C. B.; Popov, A. A.; Zhang, W. F.; Liu, F. P.; Dunsch, L. *Chem. Commun.* **2009**, 6391.
(37) Iiduka, Y.; Wakahara, T.; Nakahodo, T.; Tsuchiya, T.; Sakuraba, A.; Maeda, Y.; Akasaka, T.; Yoza, K.; Horn, E.; Kato, T.; Liu, M. T. H.; Mizorogi, N.; Kobayashi, K.; Nagase, S. *J. Am. Chem. Soc.* **2005**, *127*, 12500.
(38) Wang, T. S.; Chen, N.; Xiang, J. F.; Li, B.; Wu, J. Y.; Xu, W.; Jiang, L.; Tan, K.; Shu, C. Y.; Lu, X.; Wang, C. R. *J. Am. Chem. Soc.* **2009**, *131*, 16646.
(39) Krause, M.; Ziegs, F.; Popov, A. A.; Dunsch, L. *ChemPhysChem* **2007**, *8*, 537.
(40) Yang, H.; Lu, C.; Liu, Z.; Jin, H.; Che, Y.; Olmstead, M. M.; Balch, A. L. *J. Am. Chem. Soc.* **2008**, *130*, 17296.
(41) Mercado, B. Q.; Olmstead, M. M.; Beavers, C. M.; Easterling, M. L.; Stevenson, S.; Mackey, M. A.; Coumbe, C. E.; Phillips, J. D.; Phillips, J. P.; Poblet, J. M.; Balch, A. L. *Chem. Commun.* **2010**, *46*, 279.
(42) Valencia, R.; Rodríguez-Fortea, A.; Stevenson, S.; Balch, A. L.; Poblet, J. M. *Inorg. Chem.* **2009**, *48*, 5957.
(43) Stevenson, S.; Mackey, M. A.; Stuart, M. A.; Phillips, J. P.; Easterling, M. L.; Chancellor, C. J.; Olmstead, M. M.; Balch, A. L. *J. Am. Chem. Soc.* **2008**, *130*, 11844.
(44) Mercado, B. Q.; Stuart, M. A.; Mackey, M. A.; Pickens, J. E.; Confait, B. S.; Stevenson, S.; Easterling, M. L.; Valencia, R.; Rodríguez-Fortea, A.; Poblet, J. M.; Olmstead, M. M.; Balch, A. L. *J. Am. Chem. Soc.* **2010**, *132*, 12098.
(45) Dunsch, L.; Yang, S.; Zhang, L.; Svitova, A.; Oswald, S.; Popov, A. A. *J. Am. Chem. Soc.* **2010**, *132*, 5413.
(46) Chen, N.; Chaur, M. N.; Moore, C.; Pinzon, J. R.; Valencia, R.; Rodriguez-Fortea, A.; Poblet, J. M.; Echegoyen, L. *Chem. Commun.* **2010**, *46*, 4818.
(47) Mercado, B. Q.; Chen, N.; Rodríguez-Fortea, A.; Mackey, M. A.; Stevenson, S.; Echegoyen, L.; Poblet, J. M.; Olmstead, M. M.; Balch, A. L. *J. Am. Chem. Soc.* **2011**, *133*, 6752.
(48) (a) Rodríguez-Fortea, A.; Alegret, N.; Balch, A. L.; Poblet, J. M. *Nat. Chem.* **2010**, *2*, 955. (b) Rodríguez-Fortea, A.; Balch, A. L.; Poblet, J. M. *Chem. Soc. Rev.* **2011**, *40*, 3551. (c) Alegret, N.; Mulet-Gas, M.; Aparicio-Anglès, X.; Rodríguez-Fortea, A.; Poblet, J. M. *C. R. Chim.* **2012**, *15*, 152.
(49) Mercado, B. Q.; Beavers, C. M.; Olmstead, M. M.; Chaur, M. N.; Walker, K.; Holloway, B. C.; Echegoyen, L.; Balch, A. L. *J. Am. Chem. Soc.* **2008**, *130*, 7854.
(50) Shi, Z.-Q.; Wu, X.; Wang, C.-R.; Lu, X.; Shinohara, H. *Angew. Chem., Int. Ed.* **2006**, *45*, 2107.
(51) Kobayashi, K.; Nagase, S.; Yoshida, M.; Ōsawa, E. *J. Am. Chem. Soc.* **1997**, *119*, 12693.
(52) Slanina, Z.; Ishimura, K.; Kobayashi, K.; Nagase, S. *Chem. Phys. Lett.* **2004**, *384*, 114.
(53) Ziegler, K.; Mueller, A.; Amsharov, K. Y.; Jansen, M. *J. Am. Chem. Soc.* **2010**, *132*, 17099.
(54) Tan, Y.-Z.; Zhou, T.; Bao, J.; Shan, G.-J.; Xie, S.-Y.; Huang, R.-B.; Zheng, L.-S. *J. Am. Chem. Soc.* **2010**, *132*, 17102.
(55) Lu, X.; Nikawa, H.; Nakahodo, T.; Tsuchiya, T.; Ishitsuka, M. O.; Maeda, Y.; Akasaka, T.; Toki, M.; Sawa, H.; Slanina, Z.; Mizorogi, N.; Nagase, S. *J. Am. Chem. Soc.* **2008**, *130*, 9129.
(56) Chi, M.; Zhang, Z.; Han, P.; Fang, X.; Jia, W.; Dong, H.; Xu, B. *J. Mol. Model.* **2008**, *14*, 465.
(57) Slanina, Z.; Chen, Z.; Schleyer, P. v. R.; Uhlík, F.; Lu, X.; Nagase, S. *J. Phys. Chem. A* **2006**, *110*, 2231.
(58) Popov, A. A.; Dunsch, L. *J. Am. Chem. Soc.* **2007**, *129*, 11835.
(59) Krätschmer, W.; Lamb, L. D.; Fostiropoulos, K.; Huffman, D. R. *Nature* **1990**, *347*, 354.
(60) Fu, W.; Xu, L.; Azurmendi, H.; Ge, J.; Fuhrer, T.; Zuo, T.; Reid, J.; Shu, C.; Harich, K.; Dorn, H. C. *J. Am. Chem. Soc.* **2009**, *131*, 11762.
(61) Chen, C.; Liu, F.; Li, S.; Wang, N.; Popov, A. A.; Jiao, M.; Wei, T.; Li, Q.; Dunsch, L.; Yang, S. *Inorg. Chem.* **2012**, *51*, 3039.
(62) Popov, A. A.; Avdoshenko, S. M.; Cuniberti, G.; Dunsch, L. *J. Phys. Chem. Lett.* **2011**, *2*, 1592.
(63) Chaur, M. N.; Melin, F.; Ortiz, A. L.; Echegoyen, L. *Angew. Chem., Int. Ed.* **2009**, *48*, 7514.
(64) Yang, S. F.; Zalibera, M.; Rapta, P.; Dunsch, L. *Chem.—Eur. J.* **2006**, *12*, 7848.
(65) te Velde, G.; Bickelhaupt, F. M.; Baerends, E. J.; Fonsec Guerra, C.; van Gisbergen, S. J. A.; Snijders, J. G.; Ziegler, T. *J. Comput. Chem.* **2001**, *22*, 931.

(66) *ADF 2010.1*; Department of Theoretical Chemistry, Vrije Universiteit: Amsterdam, 2010.
(67) Becke, A. D. *Phys. Rev. A* **1988**, *38*, 3098.
(68) Perdew, J. P. *Phys. Rev. B* **1986**, *33*, 8822.